Trinity University
Digital Commons @ Trinity

Chemistry Faculty Research   Chemistry Department

2015

Impact of Size, Secondary Structure, and Counterions on the Binding of Small Ribonucleic Acids to Layered Double Hydroxide Nanoparticles

B. V. Rodriguez

J. Pescador

N. Pollok

G. W. Beall

Corina Maeder
Trinity University, cmaeder@trinity.edu

See next page for additional authors

Follow this and additional works at: https://digitalcommons.trinity.edu/chem_faculty

Part of the Chemistry Commons

Authors

B. V. Rodriguez, J. Pescador, N. Pollok, G. W. Beall, Corina Maeder, and L. K. Lewis

Impact of size, secondary structure, and counterions on the binding of small ribonucleic acids to layered double hydroxide nanoparticles

Blanca V. Rodriguez, Jorge Pescador, and Nicole Pollok
Chemistry and Biochemistry, Texas State University, 601 University Drive, San Marcos, Texas 78666

Gary W. Beall
Chemistry and Biochemistry, Texas State University, 601 University Drive, San Marcos, Texas 78666
and Physics Department, Faculty of Science, King Abdulaziz University, Jeddah 21589, Saudi Arabia

Corina Maeder
Department of Chemistry, Trinity University, One Trinity Place, San Antonio, Texas 78212

L. Kevin Lewis[a]
Chemistry and Biochemistry, Texas State University, 601 University Drive, San Marcos, Texas 78666

Use of ribonucleic acid (RNA) interference to regulate protein expression has become an important research topic and gene therapy tool, and therefore, finding suitable vehicles for delivery of small RNAs into cells is of crucial importance. Layered double metal hydroxides such as hydrotalcite (HT) have shown great promise as nonviral vectors for transport of deoxyribose nucleic acid (DNA), proteins, and drugs into cells, but the adsorption of RNAs to these materials has been little explored. In this study, the binding of small RNAs with different lengths and levels of secondary structure to HT nanoparticles has been analyzed and compared to results obtained with small DNAs in concurrent experiments. Initial experiments established the spectrophotometric properties of HT in aqueous solutions and determined that HT particles could be readily sedimented with near 100% efficiencies. Use of RNA+HT cosedimentation experiments as well as electrophoretic mobility shift assays demonstrated strong adsorption of RNA 25mers to HT, with twofold greater binding of single-stranded RNAs relative to double-stranded molecules. Strong affinities were also observed with ssRNA and dsRNA 54mers and with more complex transfer RNA molecules. Competition binding and RNA displacement experiments indicated that RNA-HT associations were strong and were only modestly affected by the presence of high concentrations of inorganic anions. © 2015 American Vacuum Society.
[http://dx.doi.org/10.1116/1.4936393]

I. INTRODUCTION

Medicinal nanotechnology aims to advance the field of drug/biomolecule delivery by improving cell targeting and biocompatibility while minimizing the toxicity of the carrier. Particularly for targeted therapies, nanoparticle carriers offer the ability to bind, protect, and deliver molecules to the desired tissues. Nanoparticles can achieve controlled release of the drugs/biomolecules through changes in the physiological environment by triggers such as changes in pH levels, temperature, or via enzymatic activity.[1,2] Nanoparticles vary in size and in chemical composition, and because of the large number of nanomaterials that exist, it is of great interest to find and optimize nanoparticles that are suitable for therapeutic purposes. Optimal carriers would not only be able to deliver and release the drug/biomolecule into targeted cells, but should also be biodegradable and have an appropriate lifespan to maximize their therapeutic activity. The eventual fate of the nanoparticles is of great importance as accumulation of foreign particles can be detrimental to cells. Moreover, nanoparticles intended for biomedical applications must be nontoxic and must not elicit an immune response.

Nanoparticles differ from bulk materials in that they are defined as being ≤ 100 nm in at least one dimension.[1–5] This feature is precisely what makes them so attractive for use in a wide range of applications. Such a minute size causes nanoparticles to have high surface-area-to-mass ratios, thereby increasing their chemical reactivity. They also have an increased ability to interact with biological polymers due to their similarity in size to biological components. An efficient uptake of molecules through the cell membrane requires their size to be at or below 200 nm, thus penetration by nanoparticles is enabled by their size.[1] Additionally, nanoparticles have been shown to partake in lysosomal escape after endocytosis.[1] It is then without surprise that nanoparticles have become interesting candidates as delivery tools for drugs or biomolecules.

Nanoclays are inorganic layered silicates, usually aluminosilicates. They can either be natural clay minerals found abundantly in nature or clays that can be easily synthesized in the lab. As such, they are inexpensive and have been shown to be useful in a multitude of applications.[6–10] Two commonly studied nanoclays, hydrotalcite (HT) and

[a]Author to whom correspondence should be addressed; electronic mail: LL18@txstate.edu

montmorillonite (MMT), have high anion (100–500 mEq/100 g) or cation (80–150 mEq/100 g) exchange capacities, respectively.[8–11] This allows them to adsorb large amounts of biomolecules. MMT is classified as a cationic nanoclay due to its high exchange capacity of cations, while HT is an anionic clay capable of exchanging anions. Recently, both nanoclays have shown great promise for the delivery of biomolecules and drugs into mammalian cells.[4,6–10,12]

HT is a member of the layered double hydroxide family and has been found to be particularly promising for gene delivery and controlled drug/deoxyribose nucleic acid (DNA) release systems.[7,13–17] Similar to MMT, HT is commonly used in a variety of different applications, such as water treatment, flame-retardants, sorbents, cosmetics, and as enteric delivery vehicles for antacids.[5,8,16] HT can be described with the formula $[M^{II}_{1-x}M^{III}_{x}(OH)_2(A^{m-})_{x/m}\cdot nH_2O]$ (x = 0.2–0.4; n = 0.5–1), where M^{II} can be divalent metal cations such as Mg, Ni, and Co, M^{III} represents trivalent metal cations such as Al and Fe, and A^{m-} are exchangeable anions such as CO_3^{2-}, SO_4^{2-}, and Cl^-. HT is structurally similar to a brucite layer, $Mg(OH)_2$, as each Mg^{2+} ion is octahedrally surrounded by six OH^- ions and every octahedral subunit pair shares edges, leading the two-dimensional layer to expand infinitely.[13–16] Isomorphic substitution of Mg^{2+} ions by Al^{3+} ions gives these layers a net positive charge. This charge is balanced by the anions that are accommodated in the interlayer gallery via electrostatic bonding.[13–16] These anions are frequently also accompanied by water molecules.

HT is a strong candidate for a biodelivery system by nearly every metric: low cost, good biocompatibility, chemical versatility, anionic exchange capacity, low toxicity to mammalian cells, easy synthesis, high drug loading density and transportation, cellular uptake, and the ability to provide protection for biomolecules and drugs. Extensive studies have shown that HT can form intercalated structures with different types of anions, such as inorganic anions, complex anions, anionic polymers, drugs, and organic biochemical anions such as amino acids and nucleic acids.[13,16,18–20] These interactions occur by an anion exchange mechanism in which the anions residing in the interlayer space are replaced by the aforementioned anions.[21] This intercalation allows for the protection of drugs/biomolecules from degradation.

In addition to the reports described above, Kim *et al.* recently demonstrated that the intercalation of both methotrexate and 5-fluorouracil (5-FU) into the HT framework increases the effectiveness of tumor growth suppression.[22] The Barahuie *et al.* group successfully delivered two anticancer drugs, chlorogenic acid and protocatehuic acid, using modified hydrotalcite.[23] The adsorption capability of HT to single- and double-stranded DNA was evidenced by a previous study performed in this lab, which noted that adsorption was dependent on the conditions of synthesis of the HT as well as on the charge density of both the DNA molecules and the HT.[9] Li *et al.* successfully transfected DNA plasmids encoding the enhanced green fluorescent protein into NSC

34 (mouse motor neuron cells).[24] Delivery of ribonucleic acid (RNA) molecules into cells after intercalation into HT has not been studied as intensively as delivery of DNA, but a few studies exist.[12,15,25,26] Interestingly, Li *et al.* demonstrated that the combination of short interfering RNA (siRNA) and anticancer drugs such as 5-FU loaded onto HT enhances the delivery efficiency into cancerous cells, demonstrating a potential advantage of combining drugs with biomolecules for cancer therapy using nanoclays.[26]

RNA interference (RNAi) is a silencing mechanism that occurs in eukaryotic cells as a protein synthesis regulation event.[27–30] This process is intricately linked to the silencing that derives from microRNAs (miRNAs). miRNAs are encoded in the nucleus of cells as long double-stranded hairpin RNA molecules that are subsequently cleaved by an enzyme (Drosha) into pre-miRNA. The pre-miRNA molecule is then exported out of the nucleus to the cytoplasm by association with the enzyme exportin 5. Pre-miRNA is processed once again by another enzyme, Dicer, creating a miRNA duplex. The miRNA associates with a complex of proteins that contain catalytic activity, termed the RISC complex. The final processing events occur during the miRNA's association with RISC, where the antisense strand of the miRNA is separated from the sense strand and remains bound to the RISC complex. The antisense strand then acts as a guide to target a complementary sequence in an mRNA, blocking translation of the mRNA into a specific protein.

In vitro and *in vivo* studies have shown that RNAi therapy can be used to target single-gene diseases as well as diseases that are caused by the overexpression of specific proteins.[27–30] Similar to traditional gene therapy applications, RNAi-based therapy would benefit immensely from optimized and biocompatible nanoparticles that can efficiently deliver small synthetic noncoding RNAs into cells. Although it is important for the nanoclays to deliver genes efficiently to the nucleus for gene therapy, RNAi strategies have more leeway as it is sufficient simply to deliver siRNA into the cytoplasm where it can be incorporated into the RNAi pathway. Strides have been made in the pursuit of finding optimal nanoparticles for RNAi, but common viral and nonviral vectors have shown drawbacks, which is where the study of nanoclays as delivery vectors for RNAi-based therapies could be beneficial.

While the adsorption capability and binding mode of DNA molecules to HT have been studied using adsorption assays and structural techniques such as x-ray diffraction and SEM analysis, work on the binding of HT to RNA is limited. It is important to analyze the adsorption and binding affinities of different RNA molecules to HT as RNA interference therapy gains traction. In contrast to DNAs, even small RNA molecules can form secondary and tertiary structures that are likely to have strong effects on their affinities for the nanomaterial. A direct comparison of the adsorption of small DNA molecules versus small RNAs with and without secondary structure could reveal important factors in determining adequate nanoparticle delivery vehicles for emerging RNA-based therapies. The aim of this project was to analyze

the adsorption of small RNA molecules containing different lengths and structures to HT nanoparticles. It is hoped that this work will help accelerate the development and optimization of RNA delivery systems for RNAi-based therapy.

II. MATERIALS AND METHODS

A. Materials

Hydrotalcite ($[Mg^{2+}_{.82}Al^{3+}_{.18}(OH)_2]Cl^-_{.18}$) with a charge density of 300 mEq/100 g was prepared through precipitation followed by hydrothermal heating in a Parr reactor at 150 °C.[9] The following DNA and RNA oligonucleotides were purchased from Integrated DNA Technologies: the single-stranded (ss)DNA 25mer Pvu4a (AAATGAGTCAC CCAGATCTAAATAA), its complement cPvu4a (TTATT TAGATCTGGGTGACTCATTT), the single-stranded RNA (ssRNA) 25mer PvuRNA (AAATGAGTCACCCAGATC TAAATAA), its complement cPvuRNA (TTATTTAGA TCTGGGTGACTCATTT), the double-stranded (ds)RNA 54mer RNALoop (AAAUGAGUCACCCAGAUCUAAAU AAGUAAUUAUUUUAGAUCUGGGUGACUCAUU), and the ssRNA 54mer RNAStr8 (AAAUGAGUCACCCAGAU CUAAAUAAGUAAAAAUGAGUCACCCAGAUCUAAA UAA). Transfer RNA (tRNA) purified from *Escherichia coli* cells (Sigma-Aldrich #R8759), Tris base, sodium carbonate, and sodium sulfate were purchased from Sigma-Aldrich. Low MW DNA Ladder and double-stranded RNA (dsRNA) Ladder were purchased from New England Biolabs. Agarose was obtained from Gold Biotechnology. Boric acid was purchased from JT Baker. SYBR Gold was purchased from Invitrogen Life Sciences. Eppendorf Flex-Tubes (1.5 ml) that exhibit minimal leaching of polypropylene additives were purchased from Eppendorf.[31] All electrophoresis experiments were performed using 11 × 14 cm Horizon gel rigs (Labrepco) and an Amersham/GE Healthcare EPS 601 power supply.

B. Methods

1. UV-Vis spectroscopy

Spectroscopic absorbance measurements and scans of HT were performed using a Cary 100 Bio UV-Vis spectrophotometer or a BioRad SmartSpec 3000 spectrophotometer. For scans, a 50 µg/ml HT sample in double-deionized water (ddH$_2$O) was scanned using a wavelength range of 200–800 nm. A time-dependent spectroscopy scan was also performed on the 50 µg/ml HT sample from 200 to 300 nm. The time points measured were 0, 1, 5, 10, 20, and 30 min. Five HT samples (50, 25, 12.5, 6.25, and 3.125 µg/ml) were also scanned from 200 to 300 nm and their absorbances at 260 nm plotted into a best-fit trendline using Microsoft Excel in order to generate a standard line and equation. HT suspensions in ddH$_2$O (2, 1, 0.5, and 0.25 mg/ml) were centrifuged at 21 000 × g for 5 min, the top half of the supernatants were removed from each tube, and their absorbances at 260 nm were measured. The concentration of HT remaining in the supernatants after centrifugation was calculated using the

trendline equation relating HT concentration to absorbance produced earlier. All assays were performed using four or five replicates, and the results were averaged.

2. Double-stranded DNA/RNA preparation

To make double-stranded DNA, aliquots of 525 ng/µl Pvu4a and 525 ng/µl cPvu4a were combined, Tris (pH 7.4) was added (5 mM final), and solutions were mixed in a total volume of 1 ml to achieve a final dsDNA concentration of 1050 ng/µl. For double-stranded RNA, aliquots of 600 ng/µl PvuRNA, 600 ng/µl cPvuRNA, ddH$_2$O, and Tris (5 mM final) were mixed as before in a total volume of 1 ml for a final dsRNA concentration of 1200 ng/µl. The solutions were placed in a heating block for 5 min at 100 °C and then allowed to anneal while cooling to RT for 30 min. Confirmation of successful dsRNA and dsDNA formation was determined using gel electrophoresis with 3.5% agarose and 0.5× Tris+boric acid (TB) electrophoresis buffer. Gels were run for approximately 10 min at 350 V as described by Sanderson *et al.*[32] Gels were stained in 0.5 µg/ml ethidium bromide for 15 min. A "Low MW DNA ladder" (New England Biolabs) was run with the dsDNA samples while a "dsRNA ladder" was used for the analysis of dsRNA samples.

3. Preparation of DNA and RNA/hydrotalcite solutions for adsorption assays

HT-ssDNA solutions were typically prepared by combining 75 µl of HT (0.25, 0.5, 1, 2, or 4 mg/ml), 3 µl 750 ng/µl Pvu4a DNA and ddH$_2$O in a final volume of 150 µl. For dsDNA binding studies, 52.5 µl 50 ng/µl dsDNA (Pvu4a annealed to cPvu4a) was added to the dsDNA/HT solutions.

HT-ssRNA solutions were prepared by mixing 75 µl of HT (0.25, 0.5, 1, 2, or 4 mg/ml), 10 µl 300 ng/µl PvuRNA and ddH$_2$O in a final volume of 150 µl. For dsRNA, 30 µl 200 ng/µl dsRNA (PvuRNA annealed to cPvuRNA) was added. HT-54mer RNA binding mixtures were prepared by mixing 19 µl 300 ng/µl RNAStr8 or RNALoop with HT and ddH$_2$O in a final volume of 150 µl. For tRNA-HT assays, 10 µl *E. coli* tRNA (300 ng/µl) was added to HT in the same final volumes as above. Assay mixtures were shaken in a microcentrifuge tube shaker for 5 min and then centrifuged at 21 000 × g for 5 min at RT.

4. DNA/HT and RNA/HT adsorption analysis

Immediately after centrifugation, the top 60 µl of the supernatant of each sample was transferred to a new microcentrifuge tube. The absorbance of the unbound DNA or RNA was then measured at 260 nm. The average of four or five samples for each DNA-HT and RNA-HT series was calculated. The percentage of total nucleic acids bound to the HT was calculated by subtracting the absorbance of free nucleic acids in the supernatant from the original nucleic acid-only absorbance. The difference was then divided by the original nucleic acid-only absorbance.

5. Analysis of RNA/hydrotalcite binding using mobility shift assays

For ssRNA-HT electrophoretic mobility shift assays (EMSAs), 300 ng ssRNA was mixed with ddH$_2$O and HT (0, 0.02, 0.04, 0.08, 0.16, 0.32, or 0.64 mg/ml) in a final volume of 20 μl. dsRNA EMSAs contained 200 ng nucleic acid and HT concentrations of 0, 0.16, 0.32, 0.64, 1.28, 2.56, and 5.12 mg/ml in a final volume of 20 μl. RNALoop EMSAs contained 100 ng nucleic acid, while RNAStr8 assays contained 150 ng and both were mixed with HT concentrations of 0, 0.04, 0.08, 0.16, 0.32, and 0.64 mg/ml. tRNA EMSAs consisted of 150 ng tRNA and HT concentrations of 0, 0.16, 0.32, 0.64, 1.28, and 2.56 mg/ml. After mixing and letting the solutions incubate for 5 min at RT, 4 μl of 30% glycerol was added to give a final volume of 24 μl and 18 μl of each sample was loaded onto the gel.

The EMSA gels were designed to effectively separate small oligonucleotides using agarose gels with the parameters described by Sanderson *et al.*[32] ssRNA (25mer), dsRNA (25mer), RNALoop (54mer), and RNAStr8 (54mer) EMSAs were performed using 3.5% agarose gels while tRNA was run on a 1.2% gel. Agarose gels were made in 45–50 ml 0.5$\times$ TB buffer and 11 $\times$ 14 cm gels. All samples were run at 350 V, except tRNA, which was run at 400 V. Gels were run for only 4–10 min to minimize bound RNA off-times and to reduce band diffusion. SYBR Gold (10 000$\times$) was diluted to 4$\times$ in 40 ml water and was layered on top of the gels to completely cover them for 15 min at RT. Each gel was then destained in water with shaking for 20 min and imaged using the ProteinSimple RED gel documentation system. Band densitometry analysis for each gel was performed using IMAGEJ software (http://imagej.nih.gov/ij/) and multiple image exposures to avoid saturation. Dissociation constants (K$_D$) were calculated by transferring the data generated from IMAGEJ to Microsoft Excel and creating a best fit trendline equation. K$_D$ values were determined from three separate gels, and the results were averaged.

6. Salt competition assays and displacement

For the competition assays, 50 μl 2 mg/ml HT was mixed with 5 μl 300 ng/μl ssRNA plus 0, 1, 10, 100, or 500 mM concentrations of either sodium carbonate or sodium sulfate in a total volume of 100 μl. The displacement assays were prepared using the same amounts of RNA, ddH$_2$O, HT, and salt; however, for these experiments, the RNA, water, and HT were combined and mixed together first and the salts were added last. The samples were agitated in an automated vortex mixer for 5 min and then centrifuged for 5 min at 21 000 $\times$ g. The A$_{260}$ of each sample was measured as described above.

III. RESULTS

The overarching goal of this study was to analyze the association of RNA molecules of varying lengths and structures with the nanoclay HT. Specifically, we were interested in assessing the binding affinity of HT for different forms of RNA: ssRNA 25mers, dsRNA 25mers, dsRNA 54mers with a short 4 nt connecting loop (RNALoop), ssRNA 54mers (RNAStr8), and tRNAs (more complex dsRNAs with multiple stem-loop regions).

In a previous study, we tested the affinities of small and large DNA molecules for HT nanoparticles that had been prepared in different ways.[9] Highest binding was observed with HT that had been synthesized at elevated temperatures (80 or 150 °C) and prepared with an anion exchange capacity of 300 mEq/100 g. Therefore, all binding experiments performed in the current study used HT synthesized at 150 °C with an exchange capacity of 300 mEq/100 g. The first approach used to quantitate binding was to incubate the nucleic acids and HT together and then measure the A$_{260}$ of DNA or RNA remaining in the supernatant after centrifugation. Before performing the binding assays, it was necessary to investigate the optical and sedimentation properties of the HT to ensure that the spectroscopic analysis was accurate and not affected by potential absorbance contributions from the HT nanoparticles.

To characterize the absorbance of HT, a 50 μg/ml sample was subjected to an absorbance scan from 200 to 800 nm. The scan revealed HT absorbance over most of this range, with stronger absorbance at the lower wavelengths [Fig. 1(a)]. Because the HT nanoparticles may be capable of scattering light, some of the apparent absorbance may also be due to this phenomenon. Centrifugation binding assays typically involve the use of multiple samples whose absorbance is measured shortly after centrifugation. As a result, even though the measurements can be made quickly, not all samples are tested at the same time. HT particles naturally sediment toward the bottoms of tubes (and cuvettes) when suspended in aqueous solutions, which may increase the variability of measurements. We assessed whether taking absorbance scans at different times after addition to a cuvette would produce lower readings over time due to continuous sedimentation of the nanoclay. As seen in Fig. 1(b), the absorbance of a 50 μg/ml HT solution decreased only slightly between 0 and 30 min after addition to a cuvette. This result indicates that natural sedimentation does not appreciably affect the absorbance of HT solutions if measurements are taken relatively quickly, e.g., within 5 min or less.

HT samples were prepared in ddH$_2$O at different concentrations and their absorbances were scanned from 200 to 300 nm, revealing that the absorbance of HT is concentration dependent [Fig. 1(c)]. From this data, the A$_{260}$ at each concentration was plotted against the HT concentration and a linear relationship was observed [Fig. 1(d)]. This wavelength was chosen because DNAs and RNAs have an absorbance peak at 260 nm that is used routinely for their quantitation. The linear relationship allowed generation of a trendline equation (y = 0.002x + 0.0183) relating absorbance at 260 nm (y) to HT concentration (x). This relationship was then used in a set of experiments to find out how easily HT particles can be sedimented using a standard biochemistry laboratory microcentrifuge. The experiments used HT stock solutions of 0.25, 0.5, 1, and 2 mg/ml, which were spun for
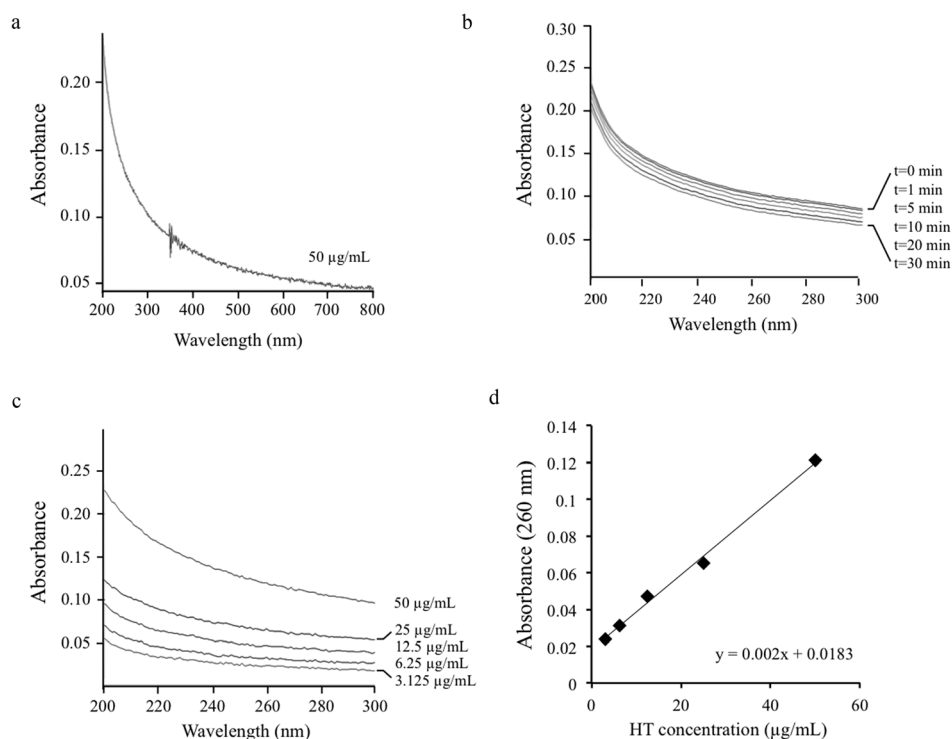
FIG. 1. Evaluation of the optical and sedimentation properties of 300–150 HT (prepared at 150 °C with exchange capacity of 300 mEq/100 g). (a) Absorbance scan of 50 μg/ml HT in ddH$_2$O; (b) Scan of a 50 μg/ml HT solution after incubation at RT in a cuvette for different times after an initial mixing step; (c) HT absorbance is concentration dependent; (d) Absorbance at 260 nm is linearly related to concentration; (e) Determination of the efficiency of sedimentation of HT particles after centrifugation for 5 min at 21 000 × g.

5 min at 21 000 × g at RT. After each spin, the A$_{260}$ of the supernatant was measured and converted to an HT concentration using the equation derived in Fig. 1(d). The data are tabulated in Fig. 1(e) and show that at the highest HT concentration, 2 mg/ml, a 5 min spin at 21 000 × g is sufficient for 99.8% of HT to be removed from the supernatant. At 0.25 and 0.5 mg/ml HT, 100% of the HT was removed. These results indicate that a 5-min spin is sufficient to sediment essentially all of the HT, and therefore, the nanoclay would not contribute substantially to absorbance measurements of nucleic acids.

The sequences and structures of the nucleic acids used in this study are shown in Figs. 2(a) and 2(b). Although the main focus of the study was to assess the binding of RNAs to HT, we included single- and double-stranded DNAs in order to have a direct comparison to a nucleic acid that has been established to have high affinity for nanoclays. The sequences of the bases in the DNA and RNA 25mers used in

the study were identical except for the natural occurrence of uracil in the RNAs and thymine in the DNAs. We used short ssRNAs, dsRNAs, and RNAs with stem-loops that mimic either siRNAs or miRNAs, which are RNA molecules involved in regulation of protein synthesis by RNA interference.[27–30] In addition, we also included tRNAs, which fold into more complex L-shaped secondary and tertiary structures.[33]

In order to investigate the adsorption of nucleic acids to HT we employed centrifugation binding assays.[8] By mixing the nucleic acids with HT in water and spinning the samples for 5 min at 21 000 × g, we were able to quantitate the amount of the free nucleic acids versus those that adsorbed to the sedimented HT by measuring the A$_{260}$ of the supernatant after the spin. In the first set of experiments, DNA and RNA 25mers were mixed with increasing amounts of HT. The percentage of DNA or RNA that became bound is plotted against HT concentration in Fig. 3(a). Averages and

A

ssDNA 25mer: **AAATGAGTCACCCAGATCTAAATAA**

dsDNA 25mer: **AAATGAGTCACCCAGATCTAAATAA**
TTTACTCAGTGGGTCTAGATTTATT

ssRNA 25mer: **AAAUGAGUCACCCAGAUCUAAAUAA**

dsRNA 25mer: **AAAUGAGUCACCCAGAUCUAAAUAA**
UUUACUCAGUGGGUCUAGAUUUAUU

ssRNA 54mer (RNAStr8):
AAAUGAGUCACCCAGAUCUAAAUAAGUAAAAAUGAGUCACCCAGAUCUAAAUAA

dsRNA 54mer (RNALoop): **AAAUGAGUCACCCAGAUCUAAAUAA**$^{G\ U}$
UUUACUCAGUGGGUCUAGAUUUAUU$_{A}$^{A}

B

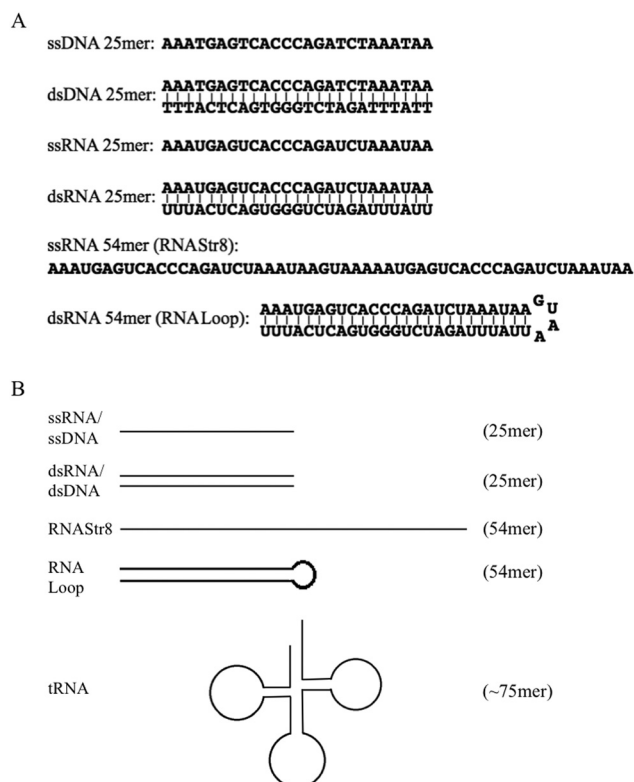|		
ssRNA/ssDNA	————————	(25mer)
dsRNA/dsDNA	————————	(25mer)
RNAStr8	————————————————	(54mer)
RNA Loop	——————○	(54mer)
tRNA		(~75mer)

FIG. 2. Sequences (a) and structural representations (b) of the different types of single- and double-stranded nucleic acids used in this study.

standard deviations from four or five assays at each concentration of HT are shown. Binding of ssDNA and ssRNA 25mers to HT was similar and substantially stronger than the binding of the double-stranded oligonucleotides over most of the range of HT concentrations used. Indeed, the percentage of bound single-stranded nucleic acids at HT concentrations from 0.2 to 1.0 mg/ml was twofold higher than that of the double-stranded molecules [Figs. 3(a) and 3(b)].

To confirm the data from the sedimentation studies in Fig. 3(a) and to determine a dissociation constant for the binding of HT to RNA, the affinity of the RNA 25mers for HT was investigated through EMSAs. EMSAs are frequently used to monitor the binding of proteins to DNA or RNA, with the nucleic acid concentration held constant while reactions are performed with increasing amounts of protein.[34] For the EMSAs with HT, 3.5% agarose gels were used in order to resolve the small RNA oligonucleotides. The gels were run at high voltages (350–400 V) with short run times (4–10 min) to minimize diffusion and to reduce opportunities for dissociation during the run. As shown in the far left lane of each gel in Fig. 3(c), free RNA migrated to the bottom of the gel and exhibited a bright band. The bright band gradually disappeared as the concentration of HT in each reaction mixture was increased. The disappearance of the free RNA band and the appearance of HT-RNA smears above the free RNA band are primarily due to the increased sizes of the HT-RNA complexes, which reduces their

a

b

Bound Nucleic Acid 25mers (%) at 1 mg/mL HT	
ssDNA	88.6
ssRNA	93.7
dsDNA	46.2
dsRNA	50.5

c

ssRNA 25mer

dsRNA 25mer

d

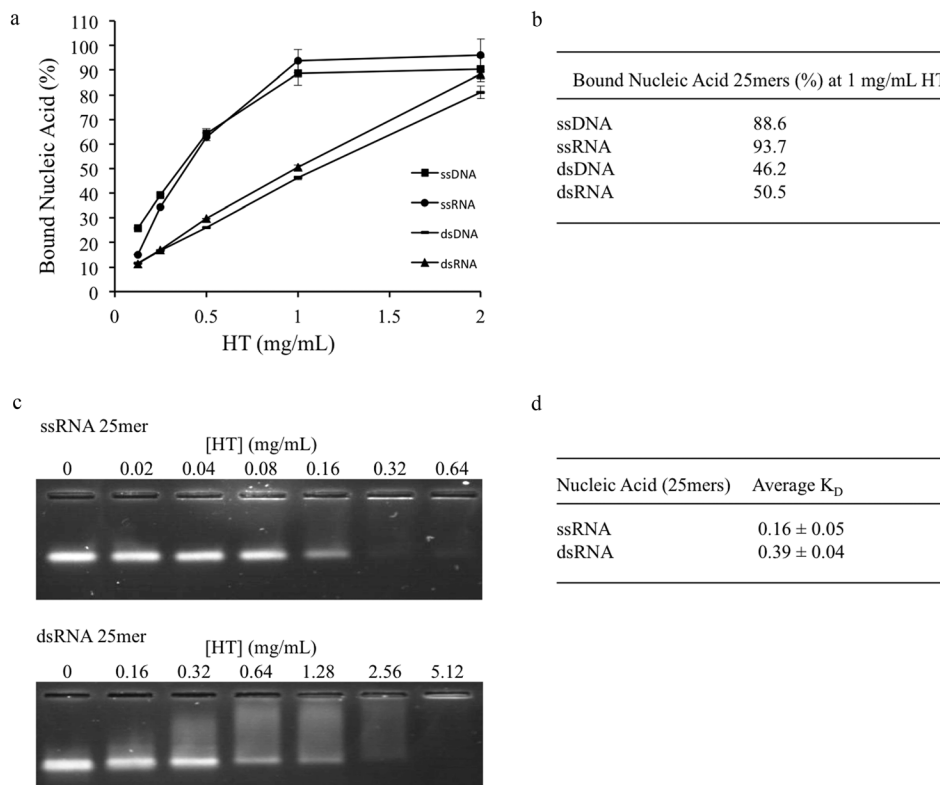| Nucleic Acid (25mers)	Average K_D
ssRNA	0.16 ± 0.05
dsRNA	0.39 ± 0.04

FIG. 3. Assessment of binding of ss and ds 25mers to HT using sedimentation assays and mobility shift assays; (a) The percentage of bound ss nucleic acids is greater than that of bound ds nucleic acids over a broad range of HT concentrations; (b) Specific percentages of bound nucleic acids at 1 mg/ml HT; (c) Representative EMSA gels run to assess adsorption of ssRNA and dsRNA 25mers; (d) K_D values (averages $\pm$ SD) calculated from three independent gels.

mobilities. As RNA became bound to the HT, which is a mixture of molecules of different sizes that have a sheetlike structure, the resulting complexes were not able to sieve efficiently through the agarose pores. When the HT concentration reached 0.16 mg/ml, more than half of the ssRNA band disappeared, indicating its association with HT. For dsRNA, the band intensity reduction to less than half of the original intensity became apparent after addition of 0.32 mg/ml HT. Densitometry analysis was performed on the bands of each EMSA gel using IMAGEJ software, the data were plotted to generate a best-fit trendline equation, and a dissociation constant (K_D) was calculated. The K_D is defined in this type of experiment as the concentration of HT at which the free RNA is reduced to 50% of initial levels, indicating that 50% of the RNA was bound to HT particles. Three or four EMSA gels were run, apparent K_D values were calculated, and the results were averaged.

HT centrifugation studies indicated a twofold higher binding affinity of ssRNA 25mers for HT compared to dsRNAs over a wide range of HT concentrations [Figs. 3(a) and 3(b)]. This twofold difference was further supported by the EMSAs, which produced a K_D of 0.16 mg/ml for HT-ssRNA and 0.39 mg/ml for HT-dsRNA complexes, roughly a twofold difference [Fig. 3(d)]. A lower K_D indicates a stronger affinity between two moieties; therefore, ssRNA displayed approximately twice the affinity for HT as dsRNA under the conditions used in the experiments.

The results from the ssRNA and dsRNA 25mer assays suggested that ssRNA had a greater affinity for HT than dsRNA over a broad range of HT concentrations. This difference could be due to the lower net negative charge on the ssRNA (-25) compared to the dsRNA (-50). Alternatively, it may be that the helical structure of the dsRNA was a factor, potentially reducing its ability to be incorporated into interlayer spaces. With these models in mind, we designed new centrifugation and EMSA assays using two RNA molecules that have the same overall negative charge but different structures. The 54mer called RNAStr8 is single-stranded and has no regions of complementary bases within itself, which prevent the formation of secondary structures [Figs. 2(a) and 2(b)]. The 54mer RNALoop was designed to spontaneously fold upon itself to form 25 bp of double-stranded RNA with a small 4 nt loop at one end, similar to a miRNA [Fig. 2(b)]. To verify the structure of RNALoop, a sample of this RNA was analyzed on a 3% agarose gel and its migration was compared to single-stranded RNAStr8. The analysis revealed that most of the RNALoop oligonucleotide was double-stranded after simply resuspending it in ddH$_2$O (Fig. 4, lane 2). After a heating and cooling step to promote annealing of complementary strands (see Sec. II B), essentially all of the RNALoop had become double-stranded (Fig. 4, lane 3).

In the initial centrifugation assays with the longer oligonucleotides, binding of the ssRNA 54mer RNAStr8 was compared to that of the ssRNA 25mer PvuRNA used in Fig. 3. The percentage of free RNA remaining in the supernatant after centrifugation is plotted against HT concentration in
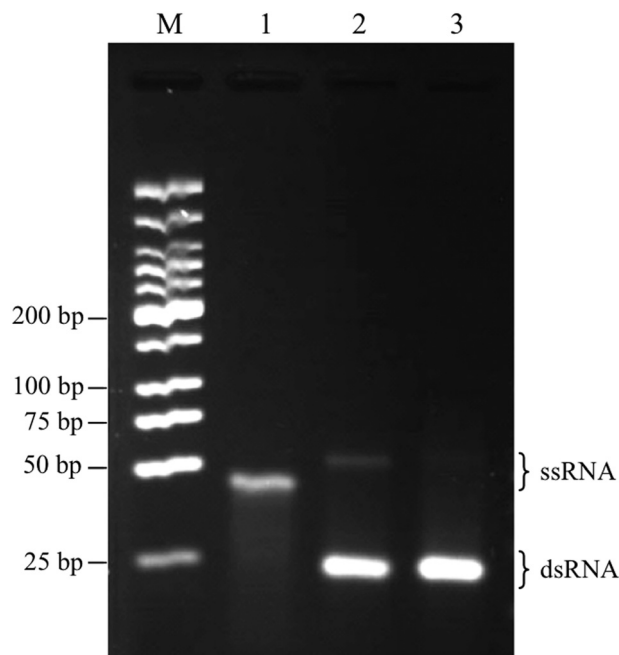

FIG. 4. Use of gel electrophoresis to confirm the double-stranded nature of RNALoop 54mers. M, low molecular weight dsDNA ladder; lane 1, RNAStr8 (ssRNA 54mer); lane 2, RNALoop (54mer capable of forming 25 bp of duplex RNA with a four nucleotide loop on one end) is mostly double-stranded after simple resuspension in ddH$_2$O; lane 3, RNALoop becomes essentially completely double-stranded in 5 mM Tris (pH 7.4) after heating at 90 °C for 4 min and cooling for 30 min at RT. The gel contained 3% agarose dissolved in 0.5× TB (Tris-borate) buffer.

Fig. 5(a). Binding of the two ssRNAs was strong and similar to each other, with greater than 85% of each RNA bound at 1 and 2 mg/ml HT. Direct comparison of binding of the ss and ds 54mers (RNAStr8 and RNALoop) revealed that, in contrast to the ss and ds 25mers, their affinities were similar to each other [Fig. 5(b)]. For example, at 1 mg/ml HT, 70.7% of the RNALoop and 85.2% of the RNAStr8 RNA was bound [Figs. 5(b) and 5(d)].

EMSA mobility shift assays indicated K_D values of 0.13 ± 0.02 for RNALoop and 0.19 ± 0.05 for RNAStr8 [Figs. 5(c) and 5(e)]. The difference in these averages was not significant because they exhibited overlapping standard deviation ranges. In summary, the centrifugation experiments indicated an 18.6% difference (70.7% vs 85.2% bound at 1 mg/ml HT) and the EMSAs pointed to a 38.8% difference (0.13 vs 0.19 K_D values) in binding affinities of the single- and double-stranded 54mers. The combined results suggest that the affinities of the single- and double-stranded 54mers for HT do not differ strongly from one another.

In addition to assessing the interactions of HT with ssRNAs and dsRNAs, we also investigated the binding affinity of HT for more complex, 75–80 nt cloverleaf-like tRNA molecules [Fig. 2(b)].[33] tRNAs participate in the translation of nucleic acids into proteins by recognizing the codons encoded in mRNA. We performed centrifugation studies using a mixture of pure *E. coli* bacterial tRNAs and the same parameters that were used for the 25mers and 54mers. Using
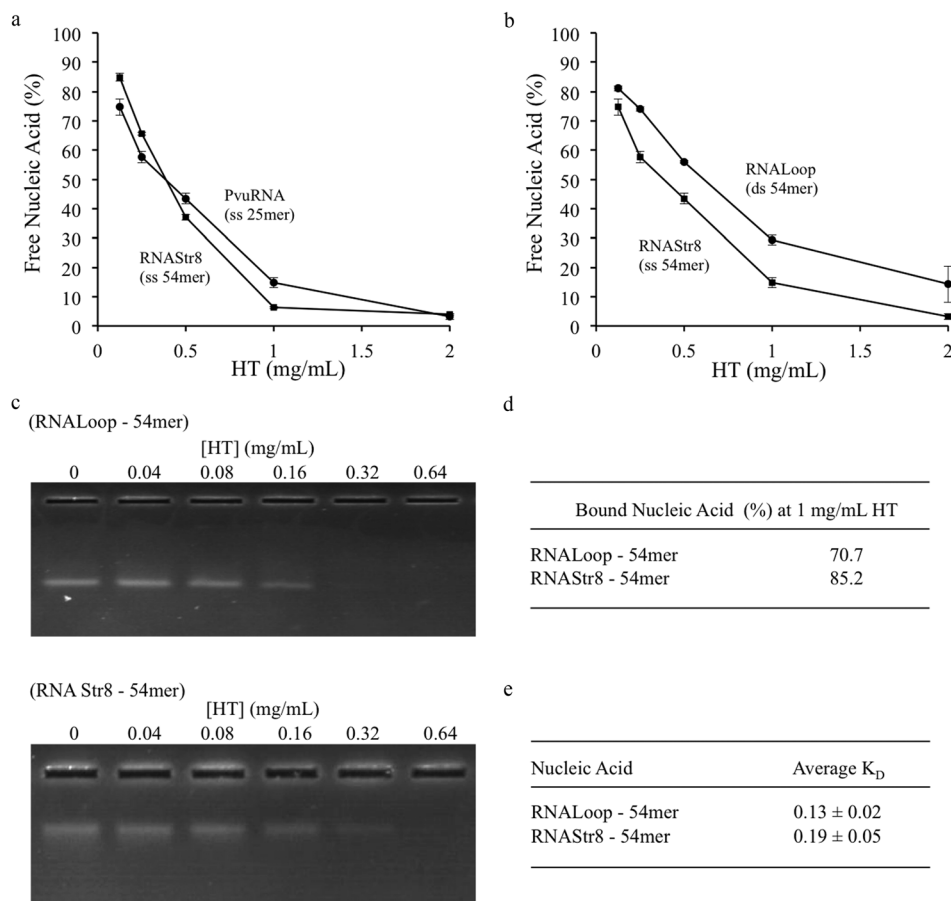
FIG. 5. HT binding studies with RNALoop and RNAStr8 54mers using centrifugation and mobility shift assays. (a) Percentage of unbound ssRNAs RNAStr8 (54mer) and PvuRNA (25mer) remaining in the supernatant after sedimentation in the presence of increasing amounts of HT; (b) Comparison of adsorption of ss 54mer RNAStr8 and ds 54mer RNALoop; (c) Representative EMSA gels performed with RNALoop (upper gel) and RNAStr8 (lower gel); (d) Specific percentage of RNALoop and RNAStr8 bound at 1 mg/ml HT using centrifugation assays; (e) K_D values (averages $\pm$ SD) calculated from three or four independent gels.

centrifugation assays, approximately 90% of the tRNA molecules became bound to HT at 1 and 2 mg/ml HT [Fig. 6(a)], which is similar to results observed with the ssRNA 25mers and 54mers. Mobility shift assays produced an average K_D of

0.21 ± 0.01 for binding of tRNAs to HT, similar to the values of 0.13 and 0.19 determined for the 54mers. A representative EMSA gel is shown in Fig. 6(b). These data show that despite having a larger and more complex three-dimensional structure
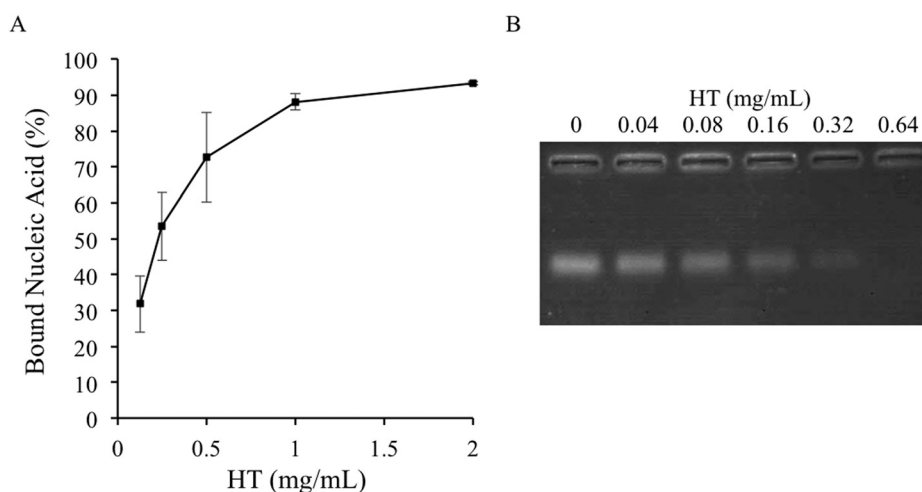

FIG. 6. Evaluation of adsorption of tRNAs containing complex folded structures to HT using (a) centrifugation binding assays and (b) EMSAs. Results from three EMSA gels were averaged to calculate a K_D of 0.210 ± 0.006.

than the RNAs tested previously, tRNAs exhibit similarly high affinities for HT.

One of the attractive features of HT as a gene delivery carrier is its ability to exchange anions from the interlayer spacing. The HT that was used in the present study contained negatively charged chlorine ions in the interlayer space, which were readily exchanged for the negatively charged nucleic acids. A past study showed that when HT containing CO_3^{2-} as the exchangeable anion is exposed to air, the anion can be exchanged with carbonate derived from atmospheric CO_2.[35] The authors of this study suggested that CO_2 most likely adsorbs to the Mg-OH sites mediated by reversible acid-base interactions.[35] The carbonate ion, being planar and divalent, binds strongly in the gallery and will displace most other anions.

Concern about anions displacing or competing off the RNA from binding to HT led us to conduct a series of centrifugation binding assays with two distinct anions, carbonate (from Na_2CO_3) and sulfate (Na_2SO_4). Competition assays were performed that involved simultaneously mixing 1 mg/ml HT with ssRNA 25mer PvuRNA (containing 5 μM RNA, corresponding to 125 μM phosphate) and increasing concentrations of sodium carbonate or sodium sulfate (1, 10, 100, or 500 mM). The percentage of free RNA in the presence and absence of the other anions is plotted against the concentration of salt added in Fig. 7(a). At the highest concentrations of added salts, 500 mM, the amount of RNA bound to HT was only reduced from 90%–95% to ~50%–60% using either salt.

Displacement studies were performed in a similar manner except that the anions were added last to the ssRNA-HT mixture, after RNA-HT complexes had already formed. Similar to the competition assays, at 500 mM anionic salt concentration, approximately 50% of the RNA molecules that had bound initially were displaced from the HT [Fig. 7(b)]. There were, however, differences at 10 and 100 mM, with carbonate having the greatest impact at these concentrations. These experiments show that anions such as carbonate

and sulfate can indeed compete with and be exchanged for RNA, but the process is inefficient, even at very high concentrations of the anions.

IV. DISCUSSION

The main goal of this study was to analyze the binding of RNA molecules with different structures to hydrotalcite. Experiments demonstrated that a simple ion-exchange assay involving centrifugation is a reliable method to measure binding of the RNAs. Although HT absorbs light at 260 nm in aqueous solutions, the nanoparticles were found to sediment exceptionally well after centrifugation in a standard microcentrifuge, and therefore, they did not interfere with A_{260} measurements of unbound RNA and DNA. It would not be expected that hydrotalcite would absorb UV light strongly, based on its structure. A possible contributor to the apparent absorbance is the trace amounts of carbonate ion that are adsorbed from the atmosphere.[35] There may also be some contribution from light scattering.

Centrifugation assays demonstrated that binding of ssRNA 25mers to HT was similar to that of ssDNAs of the same size. Binding of dsRNA and dsDNA 25mers was also similar. However, the single-stranded 25mers exhibited a twofold higher affinity for HT than the double-stranded 25mers over a broad range of HT concentrations. Electrophoretic mobility shift assays confirmed this twofold difference.

Past work by Ishihara *et al.* demonstrated that HT containing CO_3^{2-} as the exchangeable anion can exchange it with carbonate derived from atmospheric CO_2 upon exposure to air.[35] We tested the abilities of carbonate ions and sulfate ions to compete with ssRNA 25mers for binding to HT. In addition, we assessed whether bound RNAs could be easily displaced by addition of increasing concentrations of the two inorganic anions. The results revealed that the ssRNA molecules were bound tightly to the HT and, while they could be displaced, this process was inefficient and
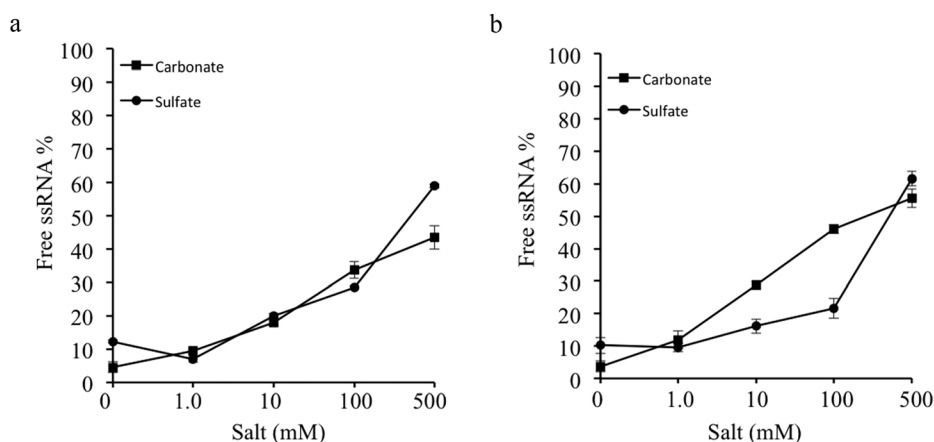

FIG. 7. Common inorganic anions compete poorly with RNA for binding to HT. Centrifugation assays were performed with ssRNA 25mers, 1 mg/ml HT, and either sodium carbonate (Na_2CO_3) or sodium sulfate (Na_2SO_4) at 0, 1, 10, 100, or 500 mM concentrations. (a) Carbonate or sulfate was added at the same time as the RNA to assess their ability to compete with ssRNA for binding to HT. (b) Assessment of the abilities of carbonate and sulfate anions to displace RNA molecules already bound to HT.

required high concentrations of the displacing anions. It is likely that the differences in binding affinities can be attributed in large part to the increased charge density and higher number of potential contacts that can be formed by the RNAs, which have 25 nucleotides, each of which contains phosphates and other functional groups that can interact with surface atoms on the HT. This phenomenon is likely to represent a cooperative effect. There are several points of interaction between the RNA and the HT; it is therefore difficult for an anion that only bonds at one site to displace the RNA completely.

Binding of the larger 54mers, RNAStr8 (ssRNA) and RNALoop (dsRNA), was also evaluated. Centrifugation assays indicated that the affinity of the ss 54mer RNAStr8 for HT was nearly identical to that of the ss 25mer PvuRNA. Furthermore, no significant difference in adsorption could be detected between ss RNAStr8 and ds RNALoop. EMSA mobility shift assays suggested that binding of RNALoop was modestly stronger than that of RNAStr8. Thus, single-stranded 25mers bound HT more strongly than double-stranded 25mers, but this structural effect on binding was not apparent when the longer 54mers were analyzed.

Centrifugation and mobility shift assays indicated that tRNAs have high affinity for HT, despite having larger and more complex structures, as well as the largest overall charge densities of the molecules tested here. At present, it is unclear if the ∼75 nt long tRNAs are binding in the same manner as the 25 and 54 nt long oligonucleotides. The possibility that some RNA species can intercalate into HT interlayer spaces while other RNAs can only bind to the surfaces or edges remains unexplored.

V. CONCLUSIONS

In this study, we have demonstrated that small RNAs bind strongly to layered double hydroxide nanoparticles, exhibiting affinities similar to those of DNA molecules. Very small single-stranded RNAs (25 nt) were found to bind to hydrotalcite with twice the affinity of double-stranded RNAs of the same length, but this ss:ds difference was not observed in longer RNA oligonucleotides. The unique ability of RNA to form simple and complex secondary structures not typically seen in DNA was also assessed; results indicated that these secondary structures did not interfere with the strong binding of the RNAs to HT. Assessing the affinities and modes of binding of small RNAs to HT is an important fundamental step in optimizing the use of this material and other nonviral vectors as carriers for RNAi therapy applications.

[1]V. Sokolova and M. Epple, Angew. Chem. **47**, 1382 (2008).
[2]A. Z. Wilczewska, K. Niemirowicz, K. H. Markiewicz, and H. Car, Pharmacol. Rep. **64**, 1020 (2012).
[3]W. H. De Jong and P. J. A. Borm, Int. J. Nanomed. **3**, 133 (2008).
[4]R. Suresh, S. N. Borkar, V. A. Sawant, V. S. Shende, and S. K. Dimble, Int. J. Pharm. Sci. Nanotechnol. **3**, 901 (2010).
[5]B. Chen, Br. Ceram. Trans. **103**, 241 (2004).
[6]J. H. Choy, S. J. Choi, J. Oh, and T. Park, Appl. Clay Sci. **36**, 122 (2007).
[7]C. Aguzzi, P. Cerezo, C. Viseras, and C. Caramella, Appl. Clay Sci. **36**, 22 (2007).
[8]G. W. Beall, D. S. Sowersby, R. D. Roberts, M. H. Robson, and L. K. Lewis. Biomacromolecules **10**, 105 (2009).
[9]B. A. Sanderson, D. S. Sowersby, S. Crosby, M. Goss, L. K. Lewis, and G. W. Beall, Biointerphases **8**, 8 (2013).
[10]F. H. Lin, C. H. Chen, W. T. Cheng, and T. F. Kuo, Biomaterials **27**, 3333 (2006).
[11]R. Pusch and R. N. Yong, *Microstructure of Smectite Clays and Engineering Performance, Spon Research* (Taylor & Francis, New York, 2006).
[12]M. Chen, H. M. Cooper, J. Z. Zhou, P. F. Bartlett, and Z. P. Xu, J. Colloid Interface Sci. **390**, 275 (2013).
[13]K. Zhang, Z. P. Xu, J. Lu, Z. Y. Tang, H. J. Zhao, D. A. Good, and M. Q. Wei, Int. J. Mol. Sci. **15**, 7409 (2014).
[14]Z. P. Xu, T. L. Walker, K. Liu, H. M. Cooper, G. M. Lu, and P. F. Bartlett, Int. J. Nanomed. **2**, 163 (2007).
[15]K. Ladewig, M. Niebert, Z. P. Xu, P. P. Gray, and G. Q. Lu, Biomaterials **31**, 1821 (2010).
[16]K. Ladewig, Z. P. Xu, and G. Q. Lu, Expert Opin. Drug Delivery **6**, 907 (2009).
[17]H. Zhang, D. Ouyang, V. Murthy, Y. Wong, Z. Xu, and S. C. Smith, Pharmaceutics **4**, 296 (2012).
[18]S. J. Choi, J. M. Oh, and J. H. Choy, J. Nanosci. Nanotechnol. **10**, 2913 (2010).
[19]P.-X. Wu, W. Li, Y.-J. Zhu, Y.-N. Tang, N.-W. Zhu, and C.-L. Guo, Appl. Clay Sci. **100**, 76 (2014).
[20]R. K. Kankala, Y. Kuthati, C.-L. Liu, and C.-H. Lee, RSC Adv. **5**, 42666 (2015).
[21]H. Nakayama, A. Hatakeyama, and M. Tsuhako, Int. J. Pharm. **393**, 105 (2010).
[22]T. H. Kim, G. J. Lee, J. H. Kang, H. J. Kim, T. I. Kim, and J. M. Oh, Biomed. Res. Int. **2014**, 193401 (2014).
[23]F. Barahuie, M. Z. Hussein, S. Gani, S. Fakarazi, and Z. Zainal, Int. J. Nanomed. **9**, 3137 (2014).
[24]S. Li, J. Li, C. J. Wang, Q. Wang, M. Z. Cader, J. Lu, D. G. Evans, X. Duan, and D. J. O'Hare, J. Mater. Chem. B **1**, 61 (2013).
[25]Y. Wong, K. Markham, Z. P. Xu, M. Chen, G. Q. Lu, P. F. Bartlett, and H. M. Cooper, Biomaterials **31**, 8770 (2010).
[26]L. Li, W. Gu, J. Chen, W. Chen, and Z. P. Xu, Biomaterials **35**, 3331 (2014).
[27]H. R. Mollaie, S. H. R. Monavari, S. A. M. Arabzadeh, M. Shamsi-Shahrabadi, M. Fazlipour, and R. M. Afshar, Asian Pac. J. Cancer Prev. **14**, 7045 (2013).
[28]K. Uchino, T. Ochiya, and F. Takeshita, Jpn. J. Clin. Oncol. **43**, 596 (2013).
[29]J. Lee, T. Yoon, and Y. Cho, Biomed. Res. Int. **2013**, 782041 (2013).
[30]B. Mansoori, S. S. Shotorbani, and B. Baradaran, Adv. Pharm. Bull. **4**, 313 (2014).
[31]L. K. Lewis, M. Robson, Y. Vecherkina, C. Ji, and G. W. Beall, Biotechniques **48**, 297 (2010).
[32]B. A. Sanderson, N. Araki, J. L. Lilley, G. Guerrero, and L. K. Lewis, Anal. Biochem. **454**, 44 (2014).
[33]K. Fujishima and A. Kanai, Front. Genet. **5**, 142 (2014).
[34]J. M. Pagano, C. C. Clingman, and S. P. Ryder, RNA **17**, 14 (2011).
[35]S. Ishihara *et al.*, JACS **135**, 18040 (2013).